

# Journal of Biomedical Optics

[SPIEDigitalLibrary.org/jbo](http://SPIEDigitalLibrary.org/jbo)

## **Ultrahigh resolution all-reflective optical coherence tomography system with a compact fiber-based supercontinuum source**

Khanh Quoc Kieu

Justin Klein

Anna Evans

Jennifer Kehlet Barton

Nasser Peyghambarian

# Ultrahigh resolution all-reflective optical coherence tomography system with a compact fiber-based supercontinuum source

Khanh Quoc Kieu,<sup>a</sup> Justin Klein,<sup>b</sup> Anna Evans,<sup>c</sup> Jennifer Kehlet Barton,<sup>b</sup> and Nasser Peyghambarian<sup>a</sup>

<sup>a</sup>University of Arizona, College of Optical Sciences, Optical Sciences Meinel Building, 1630 E. University Boulevard, Tucson, Arizona 85721

<sup>b</sup>University of Arizona, Department of Biomedical Engineering, 1657 East Helen Street, P.O. Box 210240, Tucson, Arizona 85721-0240

<sup>c</sup>Boston University, Department of Electrical and Computer Engineering, 8 Saint Mary's Street, Boston, Massachusetts 02215

**Abstract.** We report the construction and characterization of an all-reflective optical coherence tomography (OCT) system using a newly developed compact fiber-based broadband supercontinuum source. The use of only reflective optical components has enabled us to avoid chromatic dispersion effects and to obtain ultrahigh resolution OCT images of biological samples. We achieved an axial resolution of 2  $\mu\text{m}$  in air with 87 dB dynamic range at a center wavelength around 1300 nm. © 2011 Society of Photo-Optical Instrumentation Engineers (SPIE). [DOI: 10.1117/1.3633340]

Keywords: biomedical optical imaging; optical tomography; ultrahigh resolution; supercontinuum; broadband; reflective.

Paper 11175RR received Apr. 11, 2011; revised manuscript received Aug. 11, 2011; accepted for publication Aug. 16, 2011; published online Oct. 3, 2011.

## 1 Introduction

Optical coherence tomography (OCT) is an established imaging technique that allows high-resolution cross-sectional imaging of biological (and other) samples. The axial resolution in OCT scales with the bandwidth and center wavelength of the source, where higher resolution is achieved with a light source having larger spectral bandwidth and lower center wavelength.<sup>1</sup> In biological applications, scattering and water absorption, which are highly wavelength dependent, become important factors in selection of an appropriate light source. Water absorption increases with increasing wavelength and scattering increases with decreasing wavelength.<sup>2</sup> Broadband light sources having wavelengths of  $\sim 1300$  nm are especially attractive as they offer an excellent compromise between depth penetration, water absorption, and axial resolution.<sup>3</sup> Though many researchers have demonstrated impressive results in developing ultrahigh resolution OCT systems in the 1300 nm region, two challenges remain that have slowed the widespread use of these types of instruments. These challenges are the need for an inexpensive, compact, and robust broadband light source and a similarly inexpensive, compact, and robust instrument capable of using the full bandwidth of the source.

A significant research effort has been expended to develop broadband light sources that could provide ultrahigh resolution OCT at 1300 nm. Notably, axial resolution of  $\sim 2$   $\mu\text{m}$  was observed at 1300 nm using a state-of-the-art mode-locked laser.<sup>4</sup> These results were achieved by the use of complex, bulky, and expensive solid-state supercontinuum (SC) laser systems. Diode-pumped fiber sources are an interesting alternative, which combine ultrabroad bandwidth with a compact and potentially

robust and less expensive setup. Impressive results in ultrahigh resolution OCT have been demonstrated using these types of laser sources.<sup>5-7</sup> However, superluminescent diodes (SLDs) are still the dominant light source for OCT, owing to their compact size and low cost relative to solid-state SC and diode-pumped fiber lasers. Due to the limitation in spectral bandwidth that is currently obtained with these light sources (typically  $< 150$  nm), the axial resolution of OCT systems is typically  $\geq 5$   $\mu\text{m}$ . OCT with much higher resolution ( $\sim 1$   $\mu\text{m}$ ) is desirable for sub-cellular imaging and resolving the finest morphological details of samples which help to identify early stage of diseases.<sup>8</sup>

The current state of ultrahigh resolution imaging instrumentation is that the instrument must typically be custom built around the capabilities and specifications of the light source available. This includes selecting or designing custom achromatic lenses, beamsplitters, and waveplates. If the parameters of the light source, such as bandwidth or center wavelength, are changed over more than a narrow range, then optical components may need to be replaced in order to use the full bandwidth of the source. With extremely broadband sources, the system may not be able to take full advantage of the source, and the axial resolution will be larger than theoretically possible, as in Ref. 4. Another issue, in any OCT design that uses refractive elements, is the need for fine dispersion compensation which can be done in hardware or software, but in either case increases the cost and/or complexity of the system.

Here, we report a new type of SC source that is built entirely from all-fiber components made for the telecommunication industry. The laser source is thus compact and robust without any alignment or adjustment required. Furthermore, the cost of the components (excluding the pump and driving electronics) is  $\sim \$3,000$  USD and can be built in hours by personnel with minimal skill and training.<sup>9</sup> The components of the whole laser

Address all correspondence to: K. Kieu, University of Arizona, College of Optical Sciences, Optical Sciences Meinel Building, 1630 E. University Blvd. Tucson, Arizona 85721, Tel: 520-621-2382; E-mail: kkieu@optics.arizona.edu.

system are spliced together so no alignment or adjustment is required. Due to the design of the laser system it could be packaged into a handheld box. This development can help make ultrahigh resolution OCT more widespread. We incorporated this light source into an OCT system design that uses reflective components and provides ultrabroadband operation without any fine dispersion adjustment or custom achromatic optical components. The design is simple, inexpensive, and can readily accommodate  $>1000$  nm of bandwidth without adjustment or replacement of any optical components.

## 2 Materials and Methods

### 2.1 SC Laser Source

The design of the broadband SC laser source is based on an all-fiber passively mode-locked Er-doped fiber laser with carbon nanotube saturable absorber, based on a source previously described.<sup>10</sup> However, our previously designed SC laser source was not suitable for use in an OCT system and several modifications were made. A compact Er-doped all-fiber mode-locked oscillator was built using a fiber taper-based carbon nanotube saturable absorber.<sup>11</sup> The output from the oscillator was then amplified to about 100 mW, compressed in a length of SMF28 fiber, and launched into  $\sim 5$  m of dispersion shifted fiber (Vascade S1000, Corning, Corning, New York) spliced to a short segment ( $\sim 3$  cm) of highly nonlinear fiber (HNLF) (Sumitomo Electric, Hertsmere, Elstree). A fused fiber 1300/1600 wavelength-division multiplexing (WDM) coupler was spliced to the HNLF, and used as a spectral filter to remove the longer wavelength side. The WDM filter terminates in a FC/APC connector. The purpose of the dispersion shifted fiber was to stretch the pulses in time to reduce the peak power, and avoid spectral distortion when the pulses propagated through the fiber leads of the WDM filter and the output fiber. The system generates an octave-spanning supercontinuum covering a spectrum region from  $\sim 1000$  nm to beyond 2000 nm.

### 2.2 Reflective OCT System

We designed a free space all-reflective time-domain OCT system (R-OCT) to accommodate the broadband fiber laser (Fig. 1). It is well known in OCT that dispersion becomes an issue (which reduces the possible resolution of the system) when the spectral bandwidth of the light source is large. Another problem is chromatic aberration when the focusing and collimating optics are not designed to operate with very broadband light sources.<sup>12</sup> The traditional solution to deal with dispersion has been adding special glasses to one of the arms of the interferometer to compensate for the difference in dispersion in the two arms.<sup>13</sup> However, this technique adds complexity and components to the system. An all-reflective system eliminates these difficulties.

In the R-OCT system, all the reflective surfaces were either gold or silver coated to provide maximum transmission at very broad wavelengths (450 to 2000 nm). Light is introduced into the system through the output of the SC fiber source, which is placed at the focus of a 90 deg off-axis parabolic mirror (Edmund Optics, Barrington, New Jersey, NT47-096). Collimated light leaves the mirror and is split into two arms by a broadband pellicle beam splitter (Thorlabs Newton, New Jersey, BP145B3)

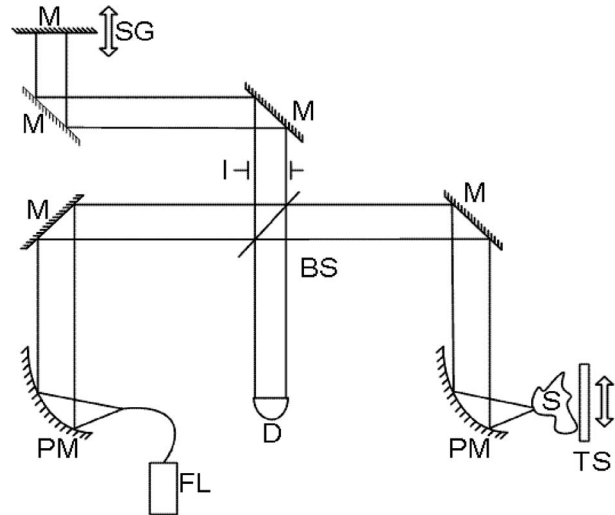


**Fig. 1** Schematic diagram of the all-reflective OCT system. BS: broadband pellicle beamsplitter; D: detector; FL: fiber laser; I: iris; M: silver coated mirror; PM: gold coated 90 deg off-axis parabolic mirror, EFL = 25.40 mm; S: sample; SG: linear scanning galvanometer; TS: translation stage.

optimized for wavelengths from 1 to  $2 \mu\text{m}$ . Reflected light passes through an iris and is steered into a reference arm consisting of a mirror mounted onto a linear scanning galvanometer (General Scanning Inc., Bedford, Massachusetts, Z193). In weakly reflecting samples, the iris can be stopped down to adjust the amount of light returning from the reference arm. Transmitted light is steered into a 90 deg off-axis parabolic mirror and was focused to a  $7 \mu\text{m}$  theoretical spot size on the sample. The sample rests on a stepper motor controlled translation stage. Light from both arms returns to the beam splitter and is split into paths reaching the detector (Newport, Irvine, California, 2011) and source. Output from the detector is fed into a lock-in amplifier (Stanford Research Instruments, Sunnyvale, California, SR810), which demodulates the signal at the Doppler frequency of the moving reference mirror. The demodulated signal is sampled by computer using a 16 bit data acquisition board (National Instruments, Austin, Texas, NI6229). Custom LABVIEW software provides an interface for data acquisition and image display.

## 3 Results

The output power of the SC source is 3 mW, the spectrum extends from  $\sim 1000$  to  $\sim 1500$  nm, has a  $\sim 1300$  nm center wavelength, and 350 nm FWHM, as shown in Fig. 2(a). The spectrum of a state-of-the-art commercial 1300 nm SLD source (Superlum, Carrigtwohill, Munster, Broadlighter:  $\lambda_c = 1295$  nm;  $\Delta\lambda = 95$  nm; coherence length =  $8 \mu\text{m}$ ) is shown in Fig. 2(b) for comparison.

The reflective system and SC source demonstrate an axial resolution of  $2 \mu\text{m}$  in air with 87 dB dynamic range. Axial resolution with the SC fiber laser source was determined from the FWHM of the point spread function (PSF) [Fig. 3(a)] which was measured to be  $\sim 2 \mu\text{m}$  in air (the resolution should be  $\sim 1.95 \mu\text{m}$  by zero phase Fourier transform of the output spectrum). The lateral resolution of the system is  $7 \mu\text{m}$ , defined by the NA of the parabolic focusing mirror. For comparison, the

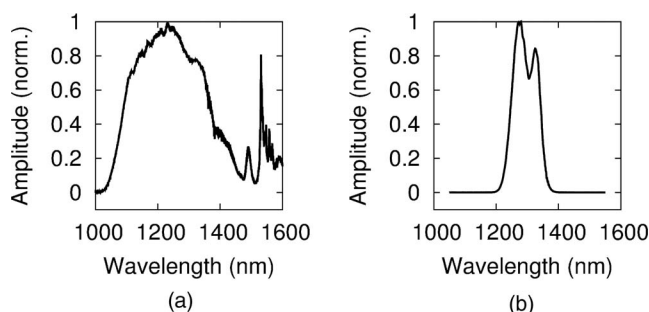


**Fig. 2** (a) Output spectrum the fiber-based supercontinuum source and (b) that of a state-of-the-art commercial SLD source.

PSF of the system using the SLD is shown in Fig. 3(b). The resolution with this source is  $\sim 8 \mu\text{m}$ , which is typical for state-of-the-art commercial SLD sources at 1300 nm. A factor of 4 improvement in resolution was observed by using the SC fiber laser source.

The dynamic range for the SC fiber laser source was determined to be 87 dB by recording images of a sample mirror with and without both arms blocked, using Eq. (1).

$$\Sigma = 20 \log_{10} \left( \frac{S_{\text{OCT}}}{\sigma} \right), \quad (1)$$

where  $\Sigma$  is the dynamic range,  $S_{\text{OCT}}$  is the maximum intensity recorded from the mirror and  $\sigma$  is the standard deviation of an image when both arms were blocked. The dynamic range measured with the SLD (4 mW output power) was similar.

### 3.1 Ex-Vivo Imaging

The all-reflective OCT system and SC fiber source were used to examine biological samples. Freshly excised mouse ear tissues were imaged with the fiber laser and commercial SLD source using the same reflective OCT system. Immediately following imaging, tissue samples were preserved in Histochoice fixative and embedded in paraffin. Histological sections were prepared and stained with hematoxylin and eosin.

Example images using both the fiber laser and the commercial SLD, as well as the matching hematoxylin and eosin (H&E) stained histological section are shown in Fig. 4. Image dimensions are  $2.53 \times 25 \text{ mm}$ .

The images demonstrate increased resolution and marked improvement in the ability to identify layers and structures

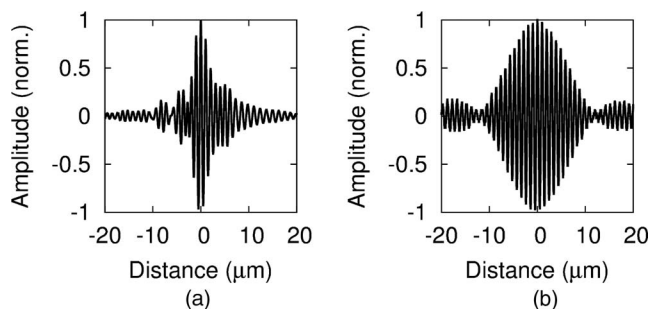


**Fig. 3** (a) PSF measured with the SC fiber laser source and (b) the commercial SLD source.

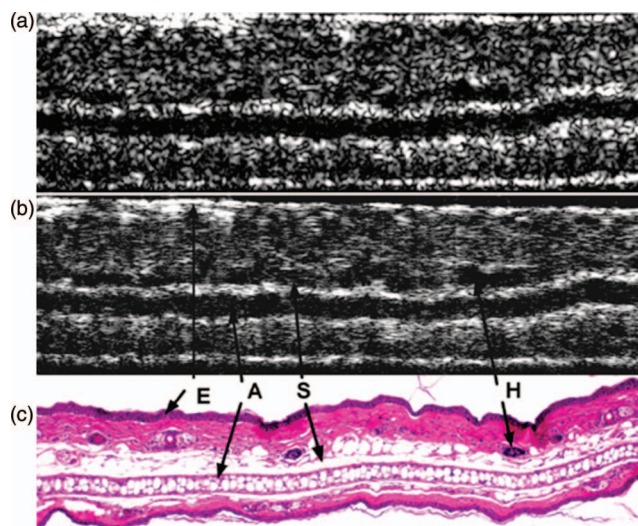


**Fig. 4** (a) OCT image acquired using the commercial SLD source. (b) OCT image acquired using the SC fiber laser source. (c) Histological image (H&E stained) of the same sample. All images are  $2.53 \times 0.25 \text{ mm}$ . A: auricular cartilage; E: epidermis; H: hair follicle; S: fatty subcutaneous layer.

within the sample tissue. In Fig. 4(a), from the commercial SLD, the epidermal layers, dermis, and auricular cartilage are easily identified. In Fig. 4(b), from the SC fiber laser, the same structures are more finely resolved and additionally, the subcutaneous layer is distinguishable from dermis. Figure 4(b) also demonstrates elongated speckles, owing to the axial resolution  $\sim 2 \mu\text{m}$  being several times better than  $\sim 7 \mu\text{m}$  lateral resolution, whereas in Fig. 4(a), axial and lateral resolution are approximately equal and speckles do not have the appearance of being elongated.

## 4 Discussion and Conclusion

We demonstrated a compact and robust SC fiber laser source that facilitated the construction of an all-reflective ultrahigh resolution OCT system. Sub- $2 \mu\text{m}$  resolution was achieved at good dynamic range. Imaging of biological samples using the developed SC fiber source has shown improvement in axial resolution and layer identification compared to a state-of-the-art commercial SLD source and is comparable to higher resolution solid-state SC sources and diode-pumped fiber lasers in terms of axial resolution. Additionally, the cost of the fiber-based SC source can be significantly less than commercially available diode-pumped lasers. Assembly of the laser does not require excessive skill or time and the resulting product is compact, reliable, and alignment free. We have also observed very good long-term stability and reliability of the laser, which has operated continuously for hundreds of hours with no deterioration in spectrum or output power. These factors make the fiber-based SC source attractive and accessible for OCT application where ultrahigh resolution is desirable.

While we recognize that other OCT systems incorporating Fourier domain techniques can be orders of magnitude faster and systems featuring balanced detection can have higher dynamic range,<sup>3</sup> the all-reflective design is still relevant. The benefit of a simple, inexpensive, and robust all-reflective de-

sign is that it could serve as a basis for improved ultrahigh resolution imaging systems, while still conferring benefits of being simple and able to transmit broad bandwidths of light ( $> 1000$  nm). Changes in the characteristics or bandwidth of light source or detection setup do not require any modification of the sampling or reference setup. A future direction for this instrument is the replacement of the single photodetector with a spectrometer setup consisting of a linescan camera and reflective diffraction grating. This enhancement will not require modification to any part of the physical setup other than the detection arm and will permit all-reflective spectral domain OCT imaging, which will significantly improve imaging speed.

### Acknowledgments

We would like to thank Masaaki Hirano of Sumitomo Electric for providing the HNLF and Photini Faith Rice for her assistance in histological processing of tissues. Support from the Center for Integrated Access Network (CIAN) is also acknowledged.

### References

1. D. Huang, E. A. Swanson, C. P. Lin, J. S. Schuman, W. G. Stinson, W. Chang, M. R. Hee, T. Flotte, K. Gregory, C. A. Puliafito, and J. G. Fujimoto, "Optical coherence tomography," *Science* **254**, 1178–1181 (1991).
2. J. M. Schmitt, A. Knüttel, M. Yadlowsky, and M. A. Eckhaus, "Optical-coherence tomography of a dense tissue: statistics of attenuation and backscattering," *Phys. Med. Biol.* **39**, 1705–1720 (1994).
3. A. F. Fercher, W. Drexler, C. K. Hitzenberger, and T. Lasser, "Optical coherence tomography—principles and applications," *Rep. Prog. Phys.* **66**, 239–303 (2003).
4. I. Hartl, X. D. Li, C. Chudoba, R. K. Ghanta, T. H. Ko, J. G. Fujimoto, J. K. Ranka, and R. S. Windeler, "Ultrahigh-resolution optical coherence tomography using continuum generation in an air-silica microstructure optical fiber," *Opt. Lett.* **26**, 608–610 (2001).
5. K. Bizheva, B. Považay, B. Hermann, H. Sattmann, W. Drexler, M. Mei, R. Holzwarth, T. Hoelzenbein, V. Wacheck, and H. Pehamberger, "Compact, broad-bandwidth fiber laser for sub-2- $\mu$ m axial resolution optical coherence tomography in the 1300-nm wavelength region," *Opt. Lett.* **28**, 707–709 (2003).
6. M. C. Stumpf, S. C. Zeller, A. Schlatter, T. Okuno, T. Südmeyer, and U. Keller, "Compact Er:Yb:glass-laser-based supercontinuum source for high-resolution optical coherence tomography," *Opt. Express* **16**, 10572–10579 (2008).
7. H. Lim, Y. Jiang, Y. Wang, Y.-C. Huang, Z. Chen, and F. W. Wise, "Ultrahigh-resolution optical coherence tomography with a fiber laser source at 1  $\mu$ m," *Opt. Lett.* **30**, 1171–1173 (2005).
8. A. Unterhuber, B. Povazay, K. Bizheva, B. Hermann, H. Sattmann, A. Stingl, T. Le, M. Seefeld, R. Menzel, M. Preusser, H. Budka, Ch Schubert, H. Reitsamer, P. K. Ahnelt, J. E. Morgan, A. Cowey, and W. Drexler, "Advances in broad bandwidth light sources for ultrahigh resolution optical coherence tomography," *Phys. Med. Biol.* **49**, 1235–1246 (2004).
9. K. Kieu, "Carbon nanotubes facilitate easy fabrication of mode-locked fiber lasers," *SPIE Newsroom* (2010).
10. K. Kieu, R. J. Jones, and N. Peyghambarian, "Generation of Few-Cycle Pulses From an Amplified Carbon Nanotube Mode-Locked Fiber Laser System," *IEEE Photonics Technol. Lett.* **22**, 1521–1523 (2010).
11. K. Kieu and M. Mansuripur, "Femtosecond laser pulse generation with a fiber taper embedded in carbon nanotube/polymer composite," *Opt. Lett.* **32**, 2242–2244 (2007).
12. A. R. Tumlinson, J. K. Barton, B. Povazay, H. Sattman, A. Unterhuber, R. A. Leitgeb, and W. Drexler, "Endoscope-tip interferometer for ultrahigh resolution frequency domain optical coherence tomography in mouse colon," *Opt. Express* **14**, 1878–1887 (2006).
13. W. Drexler, Y. Chen, A. Aguirre, B. Považay, A. Unterhuber, and J. G. Fujimoto, "Ultrahigh Resolution Optical Coherence Tomography," in *Optical Coherence Tomography*, pp. 239–279, Springer, New York (2008).